Multi-*k* spin ordering in $CaFe_3Ti_4O_{12}$ stabilized by spin-orbit coupling and further-neighbor exchange

Midori Amano Patino,[1,*] Fabio Denis Romero,[1,2] Masato Goto,[1] Takashi Saito,[1] Fabio Orlandi,[3] Pascal Manuel,[3] Attila Szabó,[3,4] Paula Kayser,[5] Ka H. Hong,[5] Khalid N. Alharbi,[5] J. Paul Attfield,[5] and Yuichi Shimakawa[1,†]

[1]*Institute for Chemical Research, Kyoto University, Uji, Kyoto 611-0011, Japan*
[2]*Hakubi Center for Advanced Research, Kyoto University, Sakyo, Kyoto 606–8501, Japan*
[3]*ISIS Facility, Rutherford Appleton Laboratory, Harwell Oxford, Didcot OX11 0QX, United Kingdom*
[4]*Department of Physics, University of Oxford, Parks Road, Oxford, OX1 3PU, United Kingdom*
[5]*Center for Science at Extreme Conditions, The University of Edinburgh, Edinburgh EH9 3FD, United Kingdom*

(Received 1 November 2020; revised 20 October 2021; accepted 2 November 2021; published 22 December 2021)

Orthogonal spin ordering is rarely observed in magnetic oxides because nearest-neighbor symmetric Heisenberg superexchange interactions usually dominate. We have discovered that in the quadruple perovskite $CaFe_3Ti_4O_{12}$, where only the $S = 2$ Fe^{2+} ion is magnetic, long-range magnetic order consisting of an unusual arrangement of three interpenetrating orthogonal sublattices is stabilized. Each magnetic sublattice corresponds to a set of FeO_4 square planes sharing a common orientation. This multi-*k* magnetic spin ordering is the result of fourth-neighbor spin couplings with a strong easy-axis anisotropy. In an applied magnetic field, each sublattice tends towards ferromagnetic alignment, but remains polarized by internal magnetic fields generated by the others, thus stabilizing in a noncollinear canted ferromagnetic structure. $CaFe_3Ti_4O_{12}$ provides a rare example of how nontrivial long-range spin order can arise when near-neighbor Heisenberg superexchange is quenched.

DOI: 10.1103/PhysRevResearch.3.043208

I. INTRODUCTION

Nontrivial spin orderings often underlie exotic physical phenomena such as high-T_C superconductivity, magnetoresistance, (multi)ferroelectricity, and topological insulating behavior [1–3]. The discovery of novel magnetic structures also has the potential to open up new avenues of research in condensed-matter physics, as well as new technological and scientific applications [4].

In the majority of complex magnetic transition-metal oxides, magnetic properties are dominated by symmetric (Heisenberg) exchange interactions which are typically orders of magnitude stronger than other interactions between magnetic centers. This tends to result in comparatively simple (anti)ferromagnetic structures [5–7]. The Hamiltonian between two magnetic centers $H = J_{ij} \sum_{\langle ij \rangle} \vec{\sigma}_i \cdot \vec{\sigma}_j$, where J_{ij} is the Heisenberg coupling between neighboring i and j spins ($\vec{\sigma}$)], is maximized for a pair of atoms with spins oriented (anti)parallel to each other. In the conventional Heisenberg model it is the sign of J_{ij} that determines the relative orientation between the spins. When an additional interaction such as antisymmetric exchange (Dzyaloshinskii-Moriya interactions) or large anisotropy becomes dominant, an unusual noncollinear structure can be stabilized [8]. These typically take place in low crystal symmetries, and therefore realizing nontrivial magnetic structures in materials with high crystal symmetry is a significant challenge [4].

The *A*-site ordered quadruple perovskites $AA'_3B_4O_{12}$ can accommodate transition-metal cations not only at the octahedral *B* site but also at the square-planar, orthogonally oriented *A*′ sites. When the *B* site is occupied by nonmagnetic cations, the complex magnetic interactions between spins at the *A*′ sites can provide a variety of nontrivial magnetic orders in the cubic crystal system [9]. For example, *A*′-site Cu^{2+} ($S = 1/2$) spins can align either ferromagnetically (FM) in $CaCu_3Ge_4O_{12}$ and $CaCu_3Sn_4O_{12}$ ($T_C = 13$ and 10 K, respectively), or antiferromagnetically (AFM) in $CaCu_3Ti_4O_{12}$ ($T_N = 25$ K) as a result of competing direct exchange and superexchange interactions [10–12]. A trend can be rationalized for related quadruple perovskite materials where increasing *A*′-site spin values leads to an increase in the magnetic transition temperature, from $10 \sim 25$ K for $S = 1/2$ (Cu^{2+} in $CaCu_3B_4O_{12}$), to 37 K for $S = 2$ (Mn^{3+} in $YMn_3Al_4O_{12}$) and 44 K for $S = 5/2$ (Mn^{2+} in $LaMn_3V_4O_{12}$) [13,14].

The material $CaFe_3Ti_4O_{12}$ is the only known quadruple perovskite where the *A*′ sites are exclusively occupied by Fe^{2+} centers with $S = 2$, yet initial studies did not find any long-range magnetic order down to 4.2 K [15,16]. This absence of magnetic ordering was notably unconventional. In this paper, we report magnetic neutron-diffraction studies on $CaFe_3Ti_4O_{12}$. We find that the $S = 2$ Fe^{2+} spins assume a complex triple-*k* antiferromagnetic order at 2.8 K. From Monte Carlo simulations, we understand this to be a consequence of strong easy-axis type anisotropy, arising from the spin-orbit coupling of the Fe^{2+} spins in the *A*′-site

*Corresponding author: amanopatino.midoriestefani.3e@kyoto-u.ac.jp
†Corresponding author: shimak@scl.kyoto-u.ac.jp

square-planar coordination. This anisotropy suppresses Heisenberg superexchange between first- and second-neighbor spins, allowing further-neighbor interactions to stabilize an orthogonal long-range spin arrangement.

II. EXPERIMENT

Polycrystalline samples of $CaFe_3Ti_4O_{12}$ were prepared from 1:3 molar-ratio mixtures of $CaTiO_3$ and $FeTiO_3$. The mixtures were ground together, packed in gold capsules, and heated at 1000 °C under 9 GPa for 6 h using a DIA cubic anvil high-pressure apparatus. Further details can be found in the Supplemental Material (SM) [17].

Neutron powder-diffraction data were collected using the POLARIS and WISH instruments at the ISIS neutron source, United Kingdom [18,19] At WISH, data were collected from a nonsintered 5.8-mm-diameter pellet of approximately 800 mg. The pellet was contained within a vanadium can where its position was fixed using a cadmium rod. Rietveld profile refinements were performed using the GSAS suite of programs [20]. Group theoretical calculations were performed using the ISODISTORT and ISOTROPY software [21,22].

^{57}Fe Mössbauer spectra were collected at 300 and 5 K from powder samples of $CaFe_3Ti_4O_{12}$ in transmission geometry with a constant-acceleration spectrometer using a ^{57}Co /Rh radiation source.

The magnetic properties of the material were measured using a Quantum Design magnetic properties measurement system (MPMS) superconducting quantum interference device magnetometer. The heat-capacity data were collected using a Quantum Design physical properties measurement system (PPMS) from a hard pellet of the $CaFe_3Ti_4O_{12}$ sample obtained by using the high-pressure apparatus (65 tons).

The Monte Carlo algorithm was used for finding different possible spin configurations in the $CaFe_3Ti_4O_{12}$ material using an in-house code [23]. Neutron powder-diffraction patterns were then calculated. Semiclassical simulation of the Hamiltonians [see Eqs. (1) and (2) below] were performed by replacing the spin operators with unit vectors and neglecting quantum entanglement. This is a good approximation for the large ($S = 2$) Fe^{2+} spins (further details in SM [17]). The powder-diffraction patterns were computed from 16 independent samples on a system comprising $32 \times 32 \times 32$ magnetic unit cells of $CaFe_3Ti_4O_{12}$ in periodic boundary conditions.

III. RESULTS AND DISCUSSION

A. Zero-field spin ground state

Neutron powder-diffraction data collected from $CaFe_3Ti_4O_{12}$ at 300 K confirm the A-site ordered quadruple perovskite structure [Fig. 1(a), Figs. S1–S3] [18,20]. The Mössbauer spectrum collected at 300 K shows a doublet for which the isomer shift and quadrupole splitting are in very good agreement with Fe^{2+} in a square-planar coordination (Fig. S4) [16]. A second small doublet corresponds to the signal of the octahedrally coordinated Fe^{2+} centers in $FeTiO_3$, which is also detected in neutron-diffraction data [approximately 4.6(1) wt. %]. These results clearly indicate Fe^{2+} at the A' sites and nonmagnetic Ti^{4+} at the B sites, yielding the charge formula $Ca^{2+}Fe_3^{2+}Ti_4^{4+}O_{12}$ [24,25].

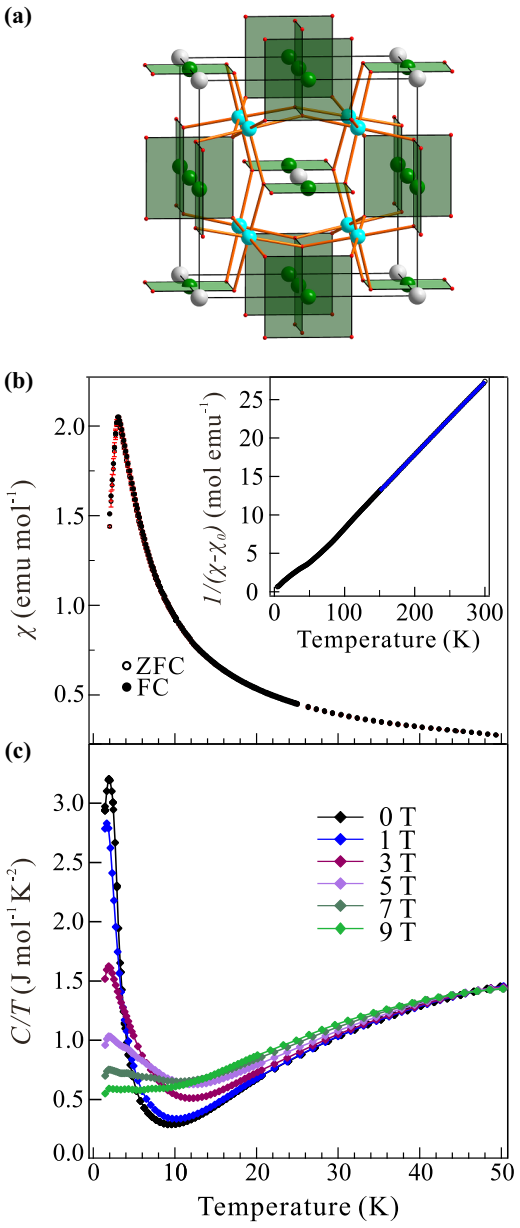

FIG. 1. (a) The crystal structure of the quadruple perovskite $CaFe_3Ti_4O_{12}$ where the calcium (A), iron (A' A'), titanium (B), and oxygen atoms are represented as white, green, blue, and red spheres, respectively. (b) ZFC and FC magnetic susceptibility data ($H = 0.01$ T). Inset shows temperature dependence of inverse magnetic susceptibility (ZFC) with the Curie-Weiss fit [solid blue line, $150 \leqslant T(K) \leqslant 300$]. (c) Heat-capacity data collected at different magnetic fields. The temperature axis T is the same for (b) and (c).

Temperature-dependent magnetic susceptibility data reveal a local maximum at 2.8 K [Fig. 1(b)]. This transition is also confirmed by a λ-type peak in heat-capacity data at 0 T [Figs. 1(c), S5]. The calculated magnetic entropy $S_m = \int (C_m/T)\, dT$ of 3.25(1) J Fe mol^{-1} K^{-1} corresponds to only 24% of the expected value for Fe^{2+} $S = 2$ [R ln5 = 13.38 J Fe mol^{-1} K^{-1}, Fig. S5(b)], indicating a considerable degree of magnetic frustration. Likewise, while the overlap of the zero field-cooled (ZFC) and field-cooled (FC) curves [Fig. 1(b)]

is consistent with antiferromagnetic ordering, a Curie-Weiss (CW) fit to the data yields $\theta_{CW} = +12.04(2)$ K from which ferromagnetic short-range correlations can be inferred [26]. Furthermore, the frustration index $|\theta_{CW}/T_N| \sim 4$ is larger than those reported for the related materials $CaCu_3Ti_4O_{12}$ ($f \sim 1.3$, G-type antiferromagnetic) and $LaMn_3V_4O_{12}$ ($f \sim 1$, helical antiferromagnetic) [14,27].

No structural changes are observed for $CaFe_3Ti_4O_{12}$ from neutron diffraction data collected down to 5 K [Fig. 2(a), Table II in SM]. [18] In contrast, data collected below the magnetic transition [$T = 1.5$ K, Fig. 2(b)] show additional peaks at the L point of the Brillouin zone [$k = (1/2, 1/2, 0)$]. These additional peaks are much broader than the nuclear reflections. From analysis of the line broadening of the magnetic reflections, we can estimate a magnetic correlation length of approximately 655 Å which corresponds to ∼44 magnetic unit cells (details in SM [17]). This short correlation length of the magnetic domains further supports magnetic frustration [28,29].

In order to solve the magnetic structure, irreducible representation analysis was used (details in Sec. 4 of the SM) [21,22,30]. From the indexed magnetic unit cell, six magnetic propagation vectors (k vectors) can be deduced from symmetry operations of the underlying point group. All solutions using one or two sets of such k vectors (arms of the star) and a single irreducible representation produce models in which only two-thirds or fewer of the Fe^{2+} sites are ordered and the magnetic moment refines to unphysically large values. A high-symmetry model was thus constructed using three arms of the star, k: (1/2, 1/2, 1), (1/2, 1, 1/2), and (1, 1/2, 1/2). The resulting triple-k ordering is shown in Fig. 3(a) (details in Table VII, SM) [31]. While the direction of the moment on each site depends on the orientation of the FeO_4 square plane, the model has only one refinable parameter: the absolute magnitude of the Fe^{2+} moment. This produces a good fit to the data [$wR_p = 4.46\%$, Fig. 2(b)]. The magnetic moment at each iron site refines to 3.78(1) μ_B, in good agreement with the 4 μ_B expected for high-spin Fe^{2+}.

The A'-site Fe^{2+} spin ground state can be described as three orthogonal interpenetrating antiferromagnetic sublattices. Each sublattice consists of Fe^{2+} spins in one of the three possible orientations of the FeO_4 planes, and orders at a different one of the three k vectors [Figs. 3(b) and 3(c)]. Each iron moment is thus orthogonal to its first and second neighbors [1NN and 2NN, Fig. 3(d)], and parallel or antiparallel to its third and fourth neighbors (3NN and 4NN).

The found dependence of the direction of the 1NN and 2NN moments with the orientation of the FeO_4 square planes is expected from strong spin-orbit coupling. The situation is similar to that observed in the $SrFeO_2$ and $Sr_3Fe_2O_5$ materials containing high-spin Fe^{2+} cations in square-planar environments. In these phases, an orbital contribution to the magnetic moment from spin-orbit coupling leads to the emergence of single-ion anisotropy [32,33]. However, in those materials the FeO_4 square planes are parallel with each other and there is no competition between single-ion anisotropy and symmetric Heisenberg exchange interactions. In contrast, in $CaFe_3Ti_4O_{12}$ the Fe^{2+} spins sit at A' sites which are orthogonally arranged in the lattice [Fig. 1(a)]. This may lead to magnetic anisotropy along a lattice-dependent direction (easy-axis anisotropy).

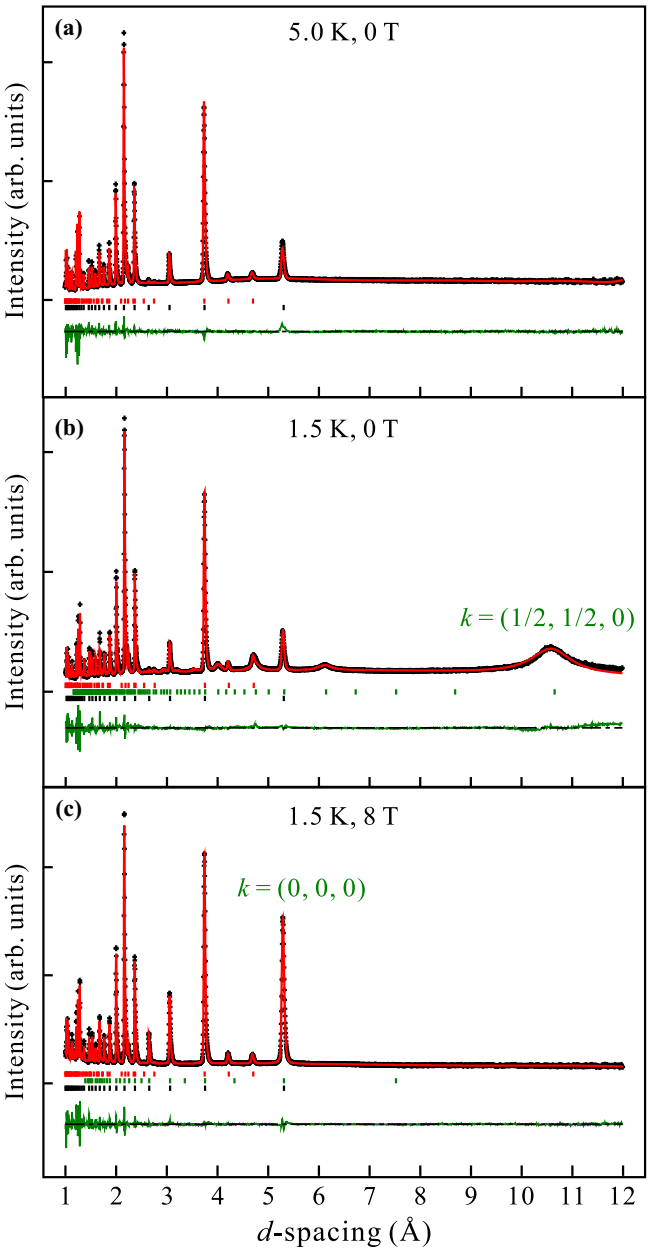

FIG. 2. Crystal and magnetic structure refinement results of $CaFe_3Ti_4O_{12}$ against neutron powder-diffraction data at (a) 5 K in zero field, (b) 1.5 K in zero field, and (c) 1.5 K in 8-T field. In all patterns, the tick marks correspond to the reflection positions of the nuclear structures of $CaFe_3Ti_4O_{12}$ (black) and $FeTiO_3$ secondary phase (4.6%, red). In (b), (c), green tick marks show the positions of the reflections corresponding to the magnetic spin structures with propagation vectors $k = (1/2, 1/2, 0)$ and $k = (0, 0, 0)$, respectively.

A neutron diffraction pattern calculated from Monte Carlo simulations of the Heisenberg exchange interactions between 1NN and 2NN spins are in effect without the influence of

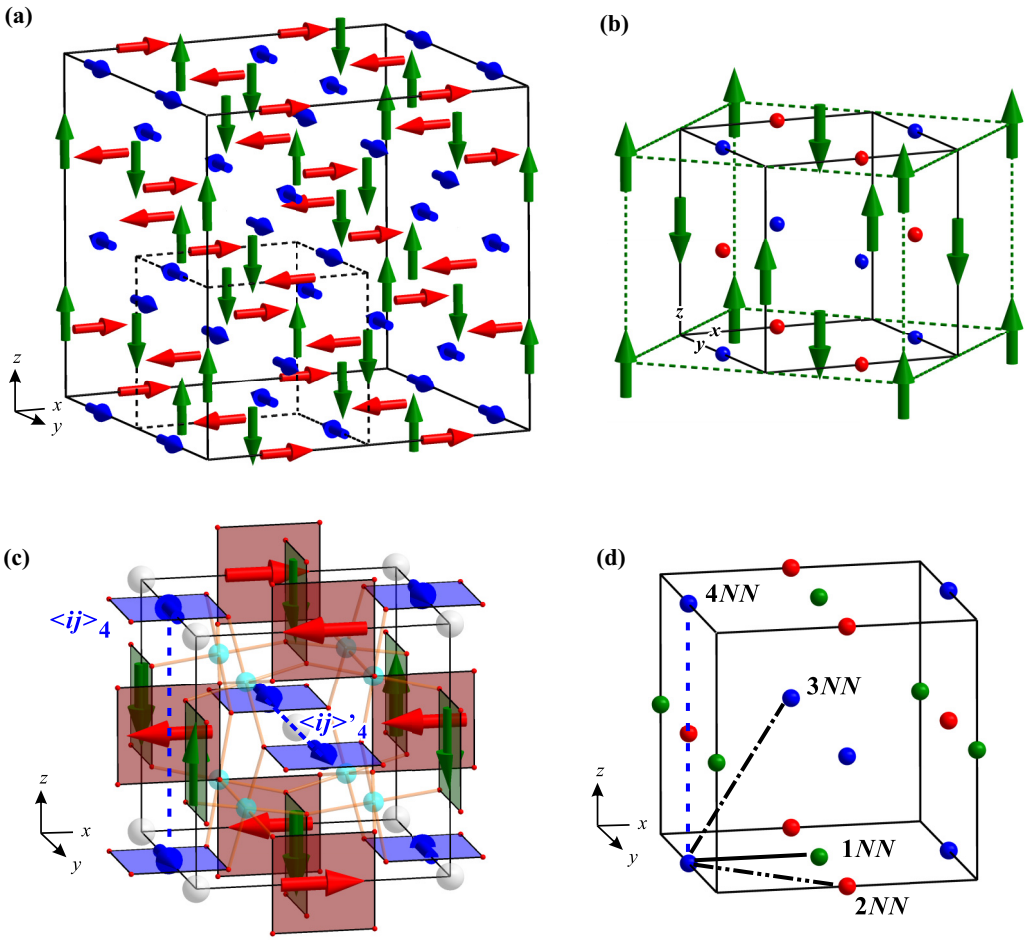

FIG. 3. (a) The antiferromagnetic structure of $CaFe_3Ti_4O_{12}$ is formed by three interpenetrating orthogonal sublattices. (b) Each sublattice orders one-third of the available Fe sites. (c) Each sublattice corresponds to the three possible orientations of the FeO_4 square planes (xy, yz, xz). (d) There are two inequivalent pathways for 4*NN* Heisenberg interaction: via Fe centers or via Ca [labeled $\langle ij\rangle_4$ and $\langle ij\rangle'_4$ in (c), respectively]. The easy axes point on the direction of the Fe-Ca-Fe $\langle ij\rangle'_4$ paths (see also Fig. S6).

easy-axis anisotropy is shown in Fig. 4. The Hamiltonian considered for this simulation is given in Eq. (1), where J_{ij} corresponds to the Heisenberg exchange integrals between $\langle ij\rangle$ neighbors and $\vec{\sigma}_i$ corresponds to the site spin.

$$H = J_1 \sum_{\langle ij\rangle} \vec{\sigma}_i \cdot \vec{\sigma}_j + J_2 \sum_{\langle ij\rangle_2} \vec{\sigma}_i \cdot \vec{\sigma}_j. \tag{1}$$

As summarized in Fig. 4, the case proposed in Eq. (1) leads to partial ordering with magnetic wave vector $k = 0$ for arbitrary values of J_1 and J_2. These features are absent in the experimental data collected from $CaFe_3Ti_4O_{12}$ [Figs. 2(b) and 4(b)], implying that 1*NN* and 2*NN* interactions do not play a significant role in the observed magnetic ground state. The simplest mechanism for the quenching of such 1*NN* and 2*NN* Heisenberg interactions is a dominant magnetic anisotropy term that fixes near-neighboring spins perpendicular to one another. The Heisenberg coupling then becomes effectively zero.

In addition to quenching nearest-neighbor Heisenberg interactions, such easy-axis anisotropy allows for 2*NN* Dzyaloshinskii-Moriya interactions. However, these do not seem to be dominant as they link the sublattices and would therefore destabilize the triple-k ordering. This leaves 3*NN* and 4*NN* interactions as the ones predominantly responsible for the long-range ordering observed. Notably, interactions between 3*NN* favor either long-range ferromagnetic or (111)/2 antiferromagnetic orders, neither of which are observed. Therefore, we believe the 3*NN* Heisenberg interactions are subleading.

The pathways of magnetic spin interaction between 4*NN* are either via an iron or a calcium center at their midpoints [Figs. 3(c) and 3(d)]. If the Fe-Fe-Fe pathways are antiferromagnetic but the Fe-Ca-Fe ones are ferromagnetic, we naturally obtain the observed (110)/2 ordering. Furthermore, the fact that the ordered moment is normal to this wave vector suggests that the easy axes point in the direction of the Fe-Ca-Fe pathway and the moments thus lie within the FeO_4 square planes as shown in Fig. 3(c).

To demonstrate that further-neighbor interactions and easy-axis anisotropy are needed to stabilize the experimentally observed triple-k ground state, Monte Carlo simulations of three cases were performed. We considered 4*NN* interactions perturbed by either: (a) 3*NN* interactions, (b) 2*NN* Dzyaloshinskii-Moriya interactions favoring an orthogonal $k = (111)/2$ order, or

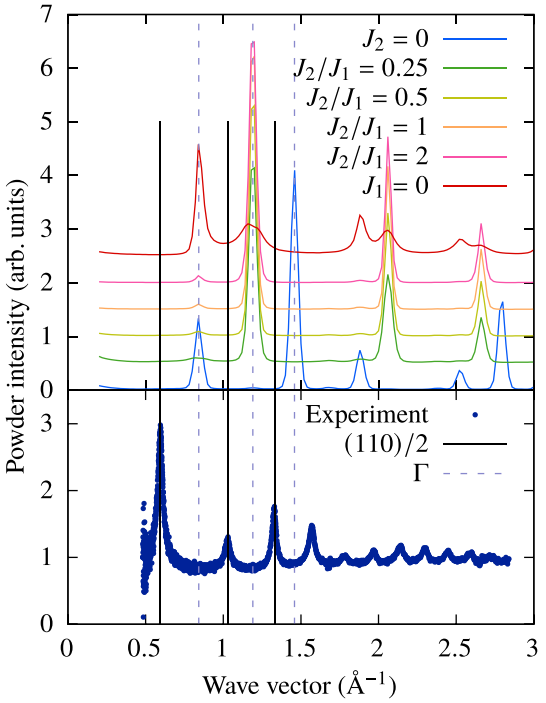

FIG. 4. Comparison of the simulations (top panel) and experimental (bottom panel) magnetic neutron-diffraction pattern for $CaFe_3Ti_4O_{12}$. The simulated pattern corresponds to the case where Heisenberg exchange integrals for 1*NN* and 2*NN* spins (J_1 and J_2) are in effect without the influence of easy-axis anisotropy (details in SM) [23]. This situation leads to partial ordering ($k = 0$) yielding the reflections indicated with gray dotted lines (Γ) which do not match the experimental data [(110)/2, solid lines].

(c) 2*NN* Dzyaloshinskii-Moriya interactions fully frustrated. The results are summarized in Fig. 5. The Hamiltonian considered is given in Eq. (2), where D_2 corresponds to the Dzyaloshinskii-Moriya interaction strength between 2*NN* spins and $A\sum_i(\vec{n}_i \cdot \vec{\sigma}_i)^2$ corresponds to the easy-axis type anisotropy term (further details in SM [17]).

$$H = J_4 \sum_{\langle ij\rangle_4} \vec{\sigma}_i \cdot \vec{\sigma}_j - J_4' \sum_{\langle ij\rangle_4'} \vec{\sigma}_i \cdot \vec{\sigma}_j - J_3 \sum_{\langle ij\rangle_3} \vec{\sigma}_i \cdot \vec{\sigma}_j + D_2 \sum_{\langle ij\rangle_2} \vec{n}_{ij} \cdot (\vec{\sigma}_i \times \vec{\sigma}_j) + A \sum_i (\vec{n}_i \cdot \vec{\sigma}_i)^2. \quad (2)$$

The $\langle ij\rangle_4$ and $\langle ij\rangle_4'$ terms in Eq. (2) denote the two 4*NN* pathways Fe-Fe-Fe and Fe-Ca-Fe, respectively [Figs. 3(c) and S6]. The easy axes n_i point in the direction of the Fe-Ca-Fe pathways $\langle ij\rangle_4'$.

In Fig. 5, the vertical solid lines indicate the position of the (110)/2 peaks arising from 4*NN* spin interactions. Sufficiently strong 3*NN* interactions (Heisenberg integral J_3) replace such (110)/2 peaks with those corresponding to the reciprocal lattice vectors [Γ in Fig. 5(a)]. The two possible D_2 contributions introduce peaks at (111)/2 and are represented with gray dotted lines [Figs. 5(b) and 5(c)].

We found that for ordered D_2, a first-order transition would be induced [$D_2 = 0.5\,J_3$, Fig. 5(b)]. The latter is not observed experimentally. Meanwhile, in the case where J_3 is

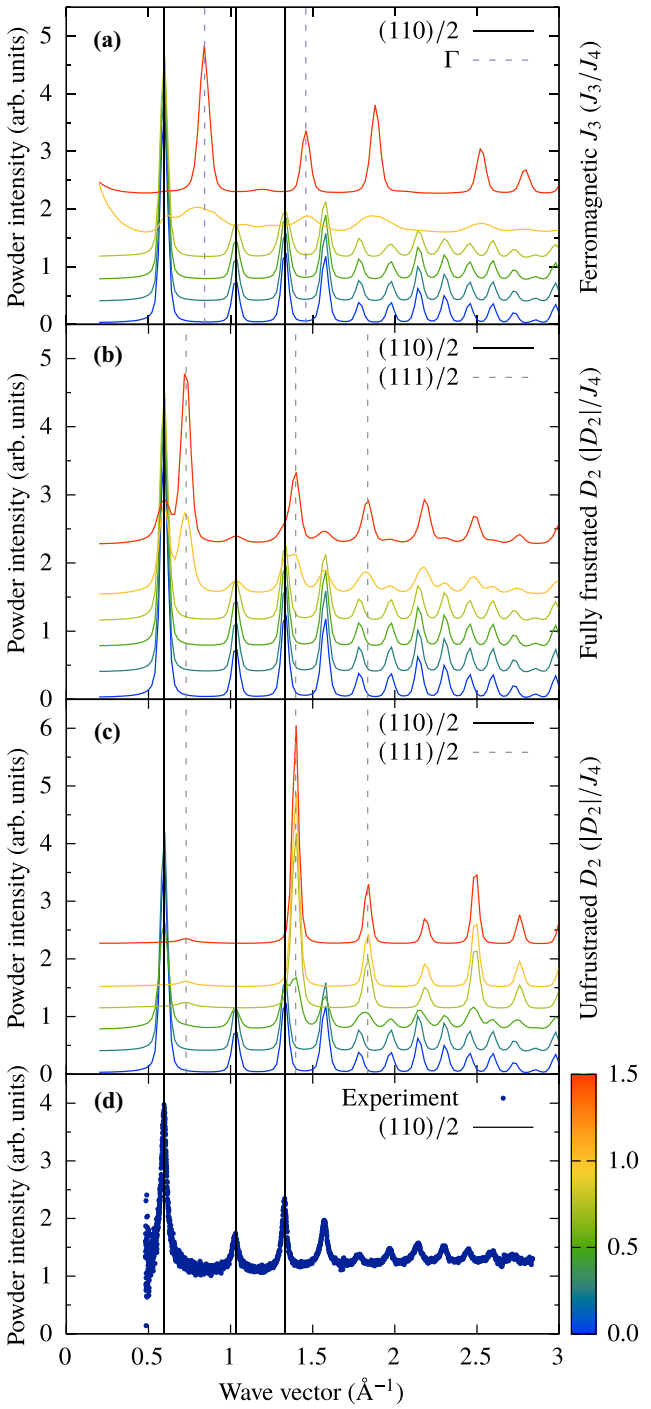

FIG. 5. Comparison of the simulations and experimental magnetic neutron powder-diffraction patterns for $CaFe_3Ti_4O_{12}$. The patterns corresponding to perturbations to J_4 by J_3 and D_2 both ordered and frustrated are presented in (a), (b), and (c) respectively. Panel (d) shows the experimental data collected at 1.5 K and 0 T. The scale bar at the right indicates the different values considered for the parameters J_3/J_4 and $|D_2|/J_4$ for the patterns in (a), and (b), (c), respectively.

active and D_2 are fully frustrated, the (110)/2 peaks would be present even at very strong perturbations and would coexist with the peaks arising from such perturbations [Fig. 5(c)]. Thus, the triple-k spin ordering remains robust even for 2*NN*

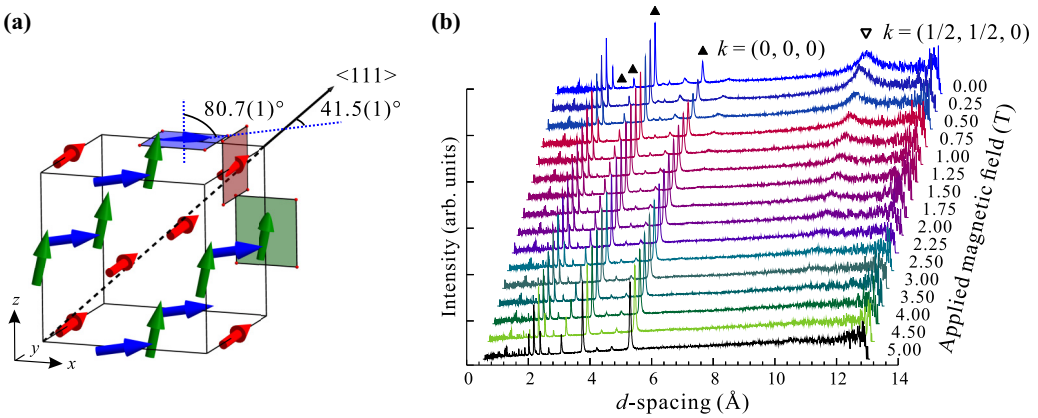

FIG. 6. (a) The refined high-field canted ferromagnetic structure of $CaFe_3Ti_4O_{12}$. (b) Neutron powder-diffraction data collected at 1.5 K under various applied magnetic fields. An increase in intensity (from $H \geqslant 0.25$ T) of the $k = (0, 0, 0)$ magnetic reflections and concomitant gradual decrease of the $k = (1/2, 1/2, 0)$ are observed.

Dzyaloshinskii-Moriya and 3*NN* Heisenberg exchange interactions of comparable magnitude to the Heisenberg exchange interactions between 4*NN* spins.

The transition temperature does not shift significantly from that corresponding to the cubic-lattice Ising value of 4.5 J_4. Therefore, we can give a fairly confident estimate of $J_4 = 2.8/4.5$ K $= 0.62$ K with slight differences expected between J_4 along inequivalent paths.

We note that the dominant 4*NN* interactions result in 3*NN* neighbors arranged both ferromagnetically and antiferromagnetically [see vectors on paths $\langle ij\rangle_4$ and $\langle ij\rangle_4'$ in Fig. 3(c)]. This frustration may contribute to the observed short magnetic correlation length. Furthermore, this ground state stabilized by further-neighbor interactions explains the much lower ordering temperature for $CaFe_3Ti_4O_{12}$ compared to those of other A'-site magnetic isostructural materials [13,14].

B. Field-induced spin structure

The magnetic transition for $CaFe_3Ti_4O_{12}$ is significantly suppressed under magnetic fields. The intensity of the C/T vs T maximum at 2.8 K decreases with increasing field and the weight of the peak integral broadens towards higher temperatures [Fig. 1(c)]. Neutron-diffraction data collected at 1.5 K under a field of 8 T do not contain the magnetic reflections of the antiferromagnetic structure. Instead, some nuclear reflections contain additional intensity consistent with magnetic ordering at propagation vector $k = (0, 0, 0)$ [Fig. 2(c)]. The intensity of these reflections is not well reproduced using a magnetic structure with collinear spins, either in a ferro- or ferrimagnetic configuration. However, they can be well accounted for using a magnetic structure comprising three noncollinear canted ferromagnetic sublattices [Fig. 6(a)]. Each of these ferromagnetic sublattices corresponds to a set of FeO_4 square planes with the same orientation. All spins make an angle of 80.7(1)° with the normal of their FeO_4 plane and the spins in other sublattices. The arrangement produces a net moment along ⟨111⟩ from which the spins form a relative angle of 41.5(1)° [Fig. 6(a)]. All moments in the structure are refined with only three parameters (M_x, M_y, M_z) and the refined moment per iron of 4.35(1) μ_B is again consistent with the expected value of 4 μ_B for Fe^{2+}, $S = 2$. This larger-than-expected moment may be explained from the fact that the data were collected from a polycrystalline sample which can result in an overestimation of the refined moment.

Under a field, the moment direction remains coupled to the FeO_4 square-plane direction, consistent with the strong easy-axis anisotropy and spin-orbit coupling. However, in this case, the three sublattices are ferro- rather than antiferromagnetic. This generates internal magnetic fields that serve to polarize the moments towards a common direction (⟨111⟩) and leads to their canted orientation. In agreement with the canted ferromagnetic structure, the magnetization measured at 2 K does not reach saturation even at 5 T (Fig. S7). The value of the magnetization at $T = 2$ K, $H = 5$ T reaches only 7.90(1) μ_B of the expected 12 μ_B per formula unit for a collinear ferromagnetic configuration of the spins.

Neutron-diffraction data collected from $CaFe_3Ti_4O_{12}$ under various applied magnetic fields at 1.5 K [Fig. 6(b)] confirm the gradual decrease in intensity of the antiferromagnetic $k = (1/2, 1/2, 0)$ reflections and a commensurate increase in the intensity of the canted ferromagnetic $k = (0, 0, 0)$ reflections with increasing field.

IV. CONCLUSIONS

The $S = 2$ Fe^{2+} centers at the A' sites in $CaFe_3Ti_4O_{12}$ order antiferromagnetically at $T_N = 2.8$ K. The spin configuration is a triple-k structure within a cubic crystal symmetry comprising three orthogonally interpenetrating antiferromagnetic spin sublattices. In this structure, the symmetric exchange for first- and second-neighbor spins are minimized by strong easy-axis type anisotropy arising from spin-orbit coupling of the high-spin Fe^{2+} centers in the A'-site square-planar coordination. Further-neighbor interactions are unquenched and stabilize the resulting unusual triple-k spin ground state. On application of magnetic field, the Fe^{2+} spins within each sublattice adopt ferromagnetic ordering. These spins remain coupled to the FeO_4 square-plane direction but generate an internal magnetic field that polarizes the spins of the other sublattices. As a result, a canted ferromagnetic spin structure is stabilized. This work provides important insights for the

realization of nontrivial magnetic structures in high-symmetry crystal structures.

ACKNOWLEDGMENTS

The authors acknowledge the science and technology facility council STFC (U.K.) for the provision of neutron beam time at WISH and POLARIS instruments, ISIS, U.K. We thank R. Smith and Helen Playford for assistance and discussion during collection of neutron-diffraction data at POLARIS. A.S. acknowledges the Oxford-ShanghaiTech collaboration project. This work was partly supported by Grants-in-Aid for Scientific Research (Grants No. 16H02266, No. 17F17039, No. 19H05823, No. 19K15585, No. 19K23650, and No. 20H00397) and by grants for the Integrated Research Consortium on Chemical Sciences and the International Collaborative Research Program of Institute for Chemical Research in Kyoto University from MEXT of Japan. This work was also supported by JSPS Core-to-Core Program (A) Advanced Research Networks and by the Yazaki Memorial Foundation for Science and Technology. Support was also provided by EPSRC and the Royal Society, UK.

[1] J. B. Goodenough, *Magnetism and the Chemical Bond* (Interscience Publishers, John Wiley & Sons, New York, 1963).

[2] D. I. Khomskii, *Transition Metal Compounds* (Cambridge University Press, Cambridge, 2014).

[3] M. Kargarian and G. A. Fiete, Topological Crystalline Insulators in Transition Metal Oxides, Phys. Rev. Lett. **110**, 156403 (2013).

[4] S. Ishiwata, T. Nakajima, J. H. Kim, D. S. Inosov, N. Kanazawa, J. S. White, J. L. Gavilano, R. Georgii, K. M. Seemann, G. Brandl, P. Manuel, D. D. Khalyavin, S. Seki, Y. Tokunaga, M. Kinoshita, Y. W. Long, Y. Kaneko, Y. Taguchi, T. Arima, B. Keimer, and Y. Tokura, Emergent topological spin structures in the centrosymmetric cubic perovskite $SrFeO_3$, Phys. Rev. B **101**, 134406 (2020).

[5] S. V. Vonsovskii, *Magnetism* (John Wiley & Sons, New York, 1974).

[6] Y. Kei, *Theory of Magnetism*, 1st ed. (Springer-Verlag, Berlin, 1996).

[7] R. M. White, *Quantum Theory of Magnetism*, 3rd ed. (Springer-Verlag, Berlin, (2007).

[8] T. Moriya, New Mechanisms of Anisotropic Superexchange Interaction, Phys. Rev. Lett. **4**, 228 (1960).

[9] Y. Shimakawa and M. Mizumaki, Multiple magnetic interactions in A-site-ordered perovskite-structure oxides, J. Phys.: Condens. Matter **26**, 473203 (2014).

[10] C. C. Homes, T. Vogt, S. M. Shapiro, S. Wakimoto, and A. P. Ramirez, Optical response of high-dielectric-constant perovskite-related oxide, Science **293**, 673 (2001).

[11] H. Shiraki, T. Saito, T. Yamada, M. Tsujimoto, M. Azuma, H. Kurata, S. Isoda, M. Takano, and Y. Shimakawa, Ferromagnetic cuprates $CaCu_3Ge_4O_{12}$ and $CaCu_3Sn_4O_{12}$ with a-site ordered perovskite structure, Phys. Rev. B **76**, 140403 (2007).

[12] M. Toyoda, K. Yamauchi, and T. Oguchi, Ab initio study of magnetic coupling in $CaCu_3B_4O_{12}$ (B = Ti, Ge, Zr, and Sn), Phys. Rev. B **87**, 224430 (2013).

[13] M. Toyoda, T. Saito, K. Yamauchi, Y. Shimakawa, and T. Oguchi, Superexchange interaction in the A-site ordered perovskite $YMn_3Al_4O_{12}$, Phys. Rev. B **92**, 014420 (2015).

[14] T. Saito, M. Toyoda, C. Ritter, S. Zhang, T. Oguchi, J. P. Attfield, and Y. Shimakawa, Symmetry-breaking 60o-spin order in the a -site-ordered perovskite $LaMn_3V_4O_{12}$, Phys. Rev. B **90**, 214405 (2014).

[15] K. Leinenweber and J. Parise, High-pressure synthesis and crystal structure of $CaFeTi_2O_6$, a new perovskite structure type, J. Solid State Chem. **114**, 277 (1995).

[16] W. M. Reiff, K. Leinenweber, and J. Parise, Low temperature magnetic properties of some new high-pressure perovskite phases of iron II: Observation of novel slow paramagnetic relaxation in $CaFe_2Ti_2O_6$ and $CaFe_3Ti_4O_{12}$, MRS Proc. **453**, 387 (1997).

[17] See Supplemental Material at http://link.aps.org/supplemental/10.1103/PhysRevResearch.3.043208 for details on the estimation of the magnetic coherence length.

[18] R. I. Smith, S. Hull, M. G. Tucker, H. Y. Playford, D. J. McPhail, S. P. Waller, and S. T. Norberg, The upgraded polaris powder diffractometer at the ISIS neutron source, Rev. Sci. Instrum. **90**, 115101 (2019).

[19] L. C. Chapon, P. Manuel, P. G. Radaelli, C. Benson, L. Perrott, S. Ansell, N. J. Rhodes, D. Raspino, D. Duxbury, E. Spill, and J. Norris, Wish: The new powder and single crystal magnetic diffractometer on the second target station, Neutron News **22**, 22 (2011).

[20] A. C. Larson and R. B. Von Dreele, General structure analysis system (GSAS), Los Alamos Natl. Lab. Rep. LAUR **86**, 154 (1994).

[21] H. T. Stokes, D. M. Hatch, and B. J. Campbell, *ISOTROPY Software Suite*, iso.byu.edu.

[22] B. J. Campbell, H. T. Stokes, D. E. Tanner, and D. M. Hatch, ISODISPLACE: A web-based tool for exploring structural distortions, J. Appl. Crystallogr. **39**, 607 (2006).

[23] P. Manuel, L. C. Chapon, P. G. Radaelli, H. Zheng, and J. F. Mitchell, Magnetic Correlations in the Extended Kagome $YBaCo_4O_7$ Probed by Single-Crystal Neutron Scattering, Phys. Rev. Lett. **103**, 037202 (2009).

[24] N. E. Brese, M. Okeeffe, and M. O'Keeffe, Bond-valence parameters for solids, Acta Crystallogr. Sect. B: Struct. Sci. **47**, 192 (1991).

[25] R. Shannon, Revised effective ionic radii and systematic studies of interatomic distances in halides and chalcogenides, Acta Crystallogr. Sect. A **32**, 751 (1976).

[26] S. D. Bhame, V. L. J. Joly, and P. A. Joy, Effect of disorder on the magnetic properties of $LaMn_{0.5}Fe_{0.5}O_3$, Phys. Rev. B **72**, 054426 (2005).

[27] Y. Shimakawa and T. Saito, A-site magnetism in a-site-ordered perovskite-structure oxides, Phys. Status Solidi Basic Res. **249**, 423 (2012).

[28] S. T. Bramwell, in *Introduction to Frustrated Magnetism*, edited by C. Lacroix, P. Mendels, and F. Mila (Springer, Berlin, 2010), pp. 45–78.

[29] D. Billington, D. Ernsting, T. E. Millichamp, C. Lester, S. B. Dugdale, D. Kersh, J. A. Duffy, S. R. Giblin, J. W. Taylor, P.

Manuel, D. D. Khalyavin, and H. Takatsu, Magnetic frustration, short-range correlations and the role of the paramagnetic fermi surface of $PdCrO_2$, Sci. Rep. **5**, 12428 (2015).

[30] A. P. Cracknell, M. F. Cracknell, and B. L. Davies, Landau's theory of second-order phase transitions and the magnetic phase transitions in some antiferromagnetic oxides, Phys. Status Solidi **39**, 463 (1970).

[31] M.-H. Whangbo, E. E. Gordon, H. Xiang, H.-J. Koo, and C. Lee, Prediction of spin orientations in terms of HOMO-LUMO interactions using spin-orbit coupling as perturbation, Acc. Chem. Res. **48**, 3080 (2015).

[32] K. Tomiyasu, H. Kageyama, C. Lee, M. H. Whangbo, Y. Tsujimoto, K. Yoshimura, J. W. Taylor, A. Llobet, F. Trouw, K. Kakurai, and K. Yamada, Magnetic excitations in infinite-layer antiferromagnetic insulator, J. Phys. Soc. Jpn. **79**, 034707 (2010).

[33] C. Tassel and H. Kageyama, Square planar coordinate iron oxides, Chem. Soc. Rev. **41**, 2025 (2012).